

# Reconfigurable Intelligent Surface (RIS): Beamforming, Modulation, and Channel Shaping

Viva Presentation

Yang Zhao, supervised by Prof Bruno Clerckx

Department of Electrical and Electronic Engineering  
Imperial College London

May 2, 2024

# Do we want more waves in the air?

Massive MIMO is here



(a) 8T8R and mMIMO at Imperial



(b) Cellular statistics

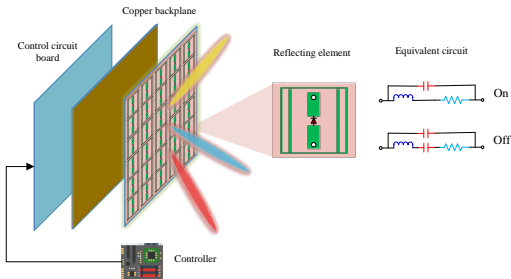
How far are we from the Shannon capacity?

$$C(\mathbf{H}) = \max_{\mathbf{Q} \succeq 0, \text{tr}(\mathbf{Q}) \leq P} \log \det \left( \mathbf{I} + \rho \mathbf{H} \mathbf{Q} \mathbf{H}^H \right)$$

- Modulation, coding, and beamforming to adapt to the stochastic channel
- Reconfigurable Intelligent Surface (RIS) can **shape and control** the channel

# What is RIS?

A planar surface of controllable scattering elements for signal amplitude and phase manipulation [1].

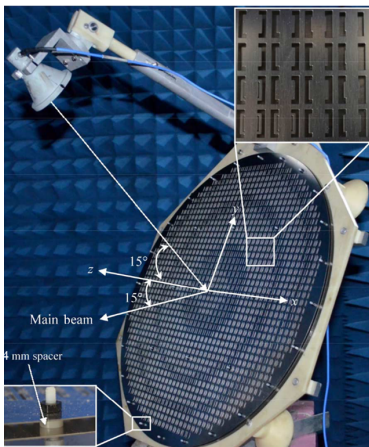


## Characteristics

- Low-power and low-cost
- Negligible noise and latency
- Full-duplex without self-interference
- Programmable in real-time

## Ancestor of RIS: Reflectarray antenna

A reflectarray antenna consists of an array illuminated by a feeding antenna [2].

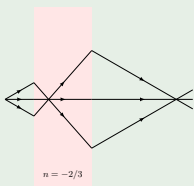


A progressive phase shift can be applied to the unit cells (a.k.a. elements) to steer the beam direction.

# What is the difference in RIS?

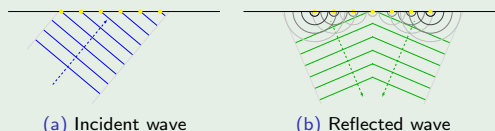
- ① Metamaterial enables **real-time control** and **unconventional behavior**.
- ② Impinging waves can be **partially refracted** and **reflected**.
- ③ The feed can be **mobile** while the surface is **scalable** and **multi-functional**.
- ④ Elements can be physically interconnected for **cooperative wave scattering**.

## Refraction



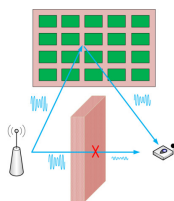
- Negative index material can focus waves
- Amplitude and phase responses can be tuned by diodes and FPGA
- Similar for wave reflection

## Reflection

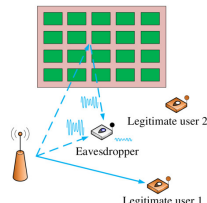


# Use case: Beamforming

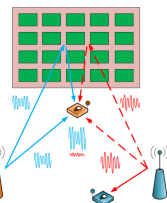
Beamforming of RIS and transceiver can be jointly designed for a specific performance measure [1].



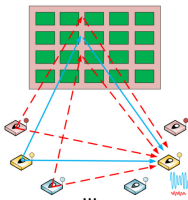
(a) Coverage extension



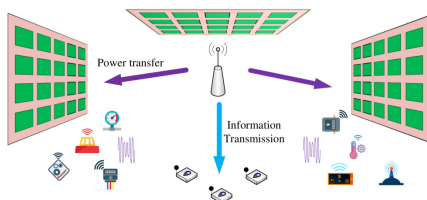
(b) Security enhancement



(c) Interference mitigation



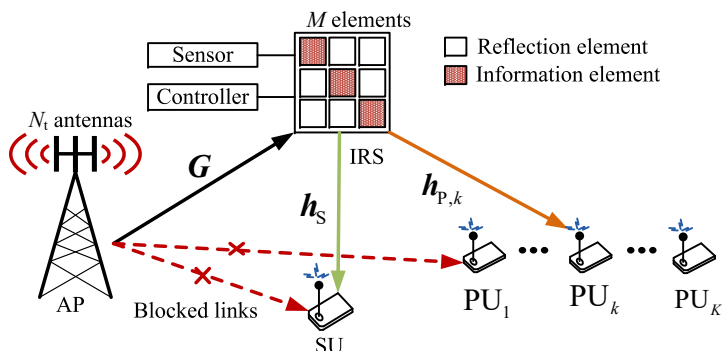
(d) Assist D2D network



(e) Assist information and power transfer

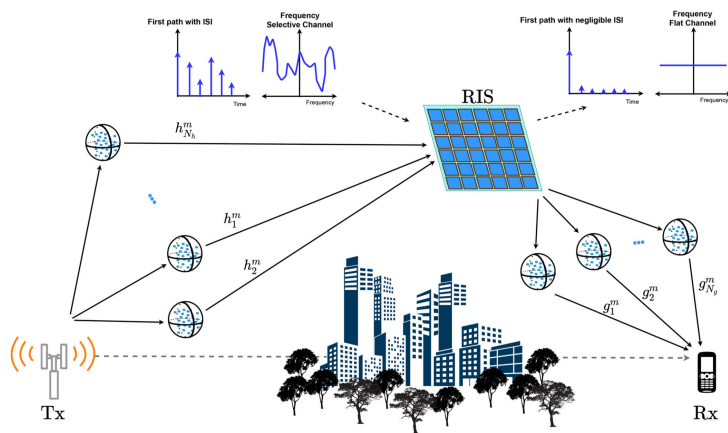
## Use case: Modulation

RIS can be used for backscatter **modulation** by periodically switching the reflection pattern [3].



## Use case: Channel shaping

Channel shaping exploits the RIS as a stand-alone device to modify the inherent properties of the propagation environment [4].



# RIS-aided SWIPT: Joint waveform and beamforming design

## Overview

- *What does this paper propose?*

A single-user multi-carrier Simultaneous Wireless Information and Power Transfer (SWIPT) system aided by a passive RIS.

- *How does it differ from previous work?*

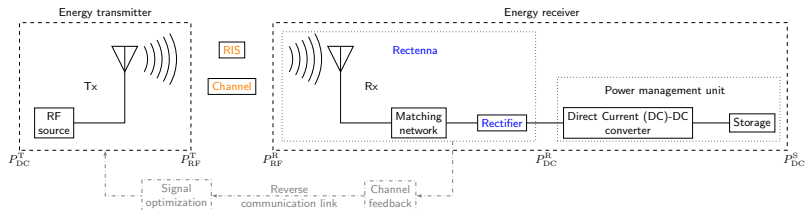
We consider waveform and beamforming design for practical receiver architectures under non-linear harvester and frequency-flat RIS models.

- *What are the benefits?*

It exploits the spatial-frequency domain and rectifier behavior to enlarge the Rate-Energy (R-E) region, achieving squared asymptotic performance than conventional designs.

# WPT via radio waves

Categories	Medium	Device	Power level	Frequency	Range
Near-field	Magnetic resonant coupling	Resonators	Up to 10 W	kHz – MHz	m
	Inductive coupling	Wire coils	Up to 10 W	Hz – MHz	cm
	Capacitive coupling	Metal plates	Up to 1 W	kHz – MHz	mm
Far-field	Radio-Frequency (RF) wave	Rectenna	$\mu\text{W} - \text{mW}$	MHz – GHz	m
	Light wave	Laser	$\mu\text{W} - \text{mW}$	THz	km



The end-to-end Wireless Power Transfer (WPT) efficiency is

$$\eta = \frac{P_{\text{DC}}^{\text{S}}}{P_{\text{DC}}^{\text{T}}} = \underbrace{\frac{P_{\text{RF}}^{\text{T}}}{P_{\text{DC}}^{\text{T}}}}_{\eta_1} \underbrace{\frac{P_{\text{RF}}^{\text{R}}}{P_{\text{RF}}^{\text{T}}}}_{\eta_2} \underbrace{\frac{P_{\text{DC}}^{\text{R}}}{P_{\text{RF}}^{\text{R}}}}_{\eta_3} \underbrace{\frac{P_{\text{DC}}^{\text{S}}}{P_{\text{DC}}^{\text{R}}}}_{\eta_4}$$

where  $\eta_2$  and  $\eta_3$  models the channel and rectenna, respectively.

# Received signal and harvested power

The rectenna efficiency  $\eta_3$  depends on its input waveform (power and shape).

## Rectenna model

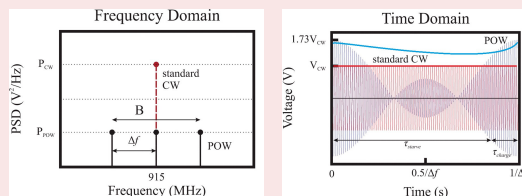
- Linear region (constant  $\eta_3$ ):  $P_{DC}^R = \eta_3 P_{RF}^R = \eta_3 \mathbb{A}\{|y(t)|^2\}$
- Non-linear region: Taylor expansion on diode characteristic equation

$$\arg_{x(t)} \max P_{DC}^R = \arg_{x(t)} \max z \triangleq \sum_{i=2, \text{even}}^{n_0} \beta_i \mathbb{A}\{y^i(t)\},$$

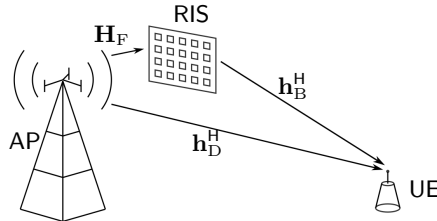
where  $\beta_i = I_S \frac{R_A^{i/2}}{i!(nv_T)^i}$  is a constant and  $n_0$  is the truncation order.

## In multi-carrier WPT ...

- $n_0 \geq 4$  allows components to compensate each other for higher DC power
- High Peak-to-Average Power Ratio (PAPR) (e.g., multi-sine) is preferred [5]



# From WPT to RIS-aided SWIPT



- SWIPT features shared signal, spectrum, and infrastructure
- RIS enhances the RF-to-RF efficiency  $\eta_2$  which has been a major concern

## Transmit waveform

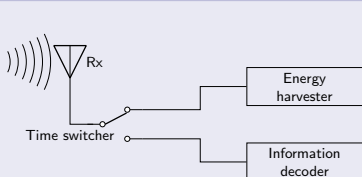
$$\mathbf{x}(t) = \Re \left\{ \sum_{n=1}^N \left( \mathbf{w}_{I,n} \cdot \underbrace{\tilde{x}_{I,n}(t) e^{j2\pi f_n t}}_{\text{modulated}} + \mathbf{w}_{P,n} \cdot \underbrace{e^{j2\pi f_n t}}_{\text{multi-sine}} \right) \right\}$$

## Frequency-flat RIS model

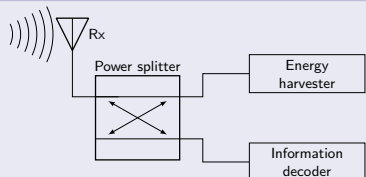
$$\mathbf{h}_n^H = \mathbf{h}_{D,n}^H + \mathbf{h}_{B,n}^H \boldsymbol{\Theta} \mathbf{H}_{F,n}$$

# Performance analysis

## Receiver architectures



(a) Time Switching (TS) receiver



(b) Power Splitting (PS) receiver

## Rate-Energy (R-E) region of PS

$$R(\boldsymbol{\theta}, \mathbf{w}_I, \rho) = \sum_{n=1}^N \log_2 \left( 1 + \frac{(1-\rho)|\mathbf{h}_n^\text{H} \mathbf{w}_{I,n}|^2}{\sigma_n^2} \right),$$

$$z(\boldsymbol{\theta}, \mathbf{w}_I, \mathbf{w}_P, \rho) = \sum_{i=2, \text{even}}^{n_0} \beta_i \rho^{i/2} \mathbb{E} \left\{ \mathbb{A} \left\{ y^i(t) \right\} \right\},$$

$$\mathcal{C}_{\text{R-E}}(P) \triangleq \left\{ (r, e) : 0 \leq r \leq R, 0 \leq e \leq z, \|\mathbf{W}_I\|_F^2/2 + \|\mathbf{W}_P\|_F^2/2 \leq P \right\}$$

# Joint waveform and beamforming design

## Problem formulation

$$\begin{aligned} & \max_{\boldsymbol{\theta}, \mathbf{W}_I, \mathbf{W}_P, \rho} \quad z(\boldsymbol{\theta}, \mathbf{W}_I, \mathbf{W}_P, \rho) \\ \text{s.t.} \quad & \|\mathbf{W}_I\|_F^2/2 + \|\mathbf{W}_P\|_F^2/2 \leq P, \\ & R(\boldsymbol{\theta}, \mathbf{W}_I, \rho) \geq \bar{R}, \\ & |\phi_l| = 1, \quad l = 1, \dots, L, \\ & 0 \leq \rho \leq 1, \end{aligned}$$

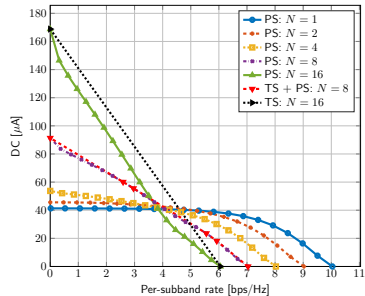
## Solution by Block Coordinate Descent (BCD)

- Optimally decouple the spatial and frequency domain design

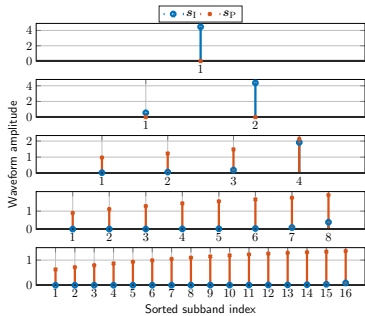
$$\mathbf{W}_{I/P,n} = \underbrace{s_{I/P,n}}_{\text{frequency}} \underbrace{\mathbf{p}_{I/P,n}}_{\text{spatial}}$$

- Active beamforming  $\mathbf{p}$ : Maximum Ratio Transmission (MRT)
- Passive beamforming  $\boldsymbol{\theta}$ : Successive Convex Approximation (SCA)
- Power allocation  $s$  and splitting ratio  $\rho$ : Geometric Programming (GP)

# Simulation results: Number of subbands $N$



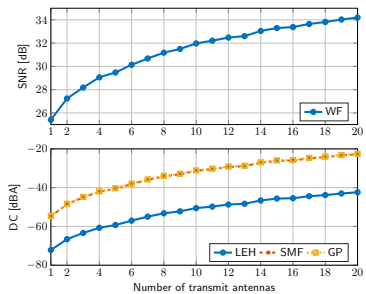
(a) R-E region



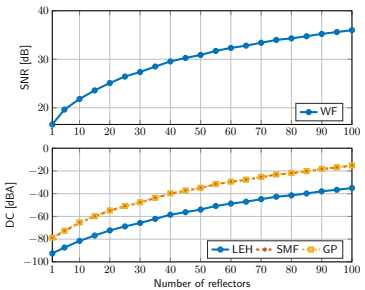
(b) Waveform amplitude

- Increasing  $N$  reduces per-subband rate but boosts harvested energy
- Region is convex at small  $N$  (favors PS) and concave at large  $N$  (favors TS)
- Dedicated multi-sine power waveform is unnecessary at small  $N$

## Simulation results: Asymptotic behavior



(a) Number of transmit antennas  $M$



(b) Number of RIS elements  $L$

- Active beamforming: array gain  $M$  and harvested power order  $M^2$
- Passive beamforming: array gain  $L^2$  and harvested power order  $L^4$
- Superlinear thanks to coherent scattering and rectifier nonlinearity

# RISscatter: Unifying Backscatter Communication (BackCom) and RIS

## Overview

- *What does this paper propose?*

RISscatter — a batteryless cognitive radio that recycles ambient signal in an adaptive and customizable manner.

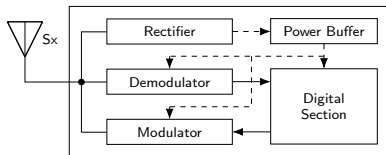
- *How does it differ from previous work?*

Backscatter modulation and passive beamforming are seamlessly integrated from the perspective of probability distribution.

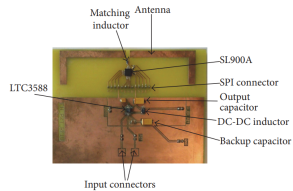
- *What are the benefits?*

It supports cooperative and distributed deployment, avoids complex architecture and signal processing, and can be built over legacy systems.

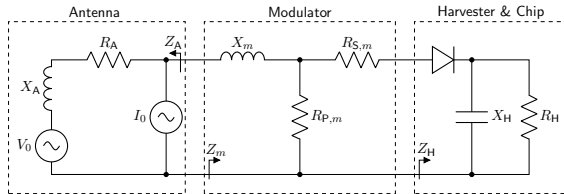
# Node architecture



(a) Block Diagram



(b) RFID tag with harvester [6]



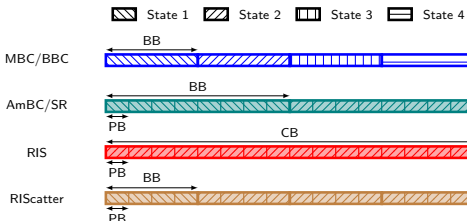
(c) Equivalent Circuit

Impinging waves can be used for powering, modulation, and beamforming.

# Reflection coefficient

The node changes state by switching load impedance (and reflection coefficient)

$$\Gamma = \frac{Z_L - Z_0^*}{Z_L + Z_0}$$



- RIS: the state at a specific time is known (as a passive beamforming codeword) to the transceiver

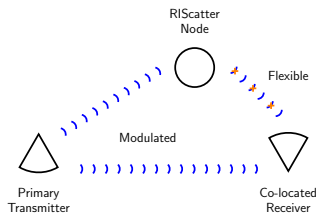
$$\Gamma_m = \exp(j\phi_m),$$

- BackCom: all states occur with equal probability (as part of information codeword) to be detected at the receiver

$$\Gamma_m = \alpha_m \frac{c_m}{\max_{m'} |c_{m'}|},$$

# RISscatter system

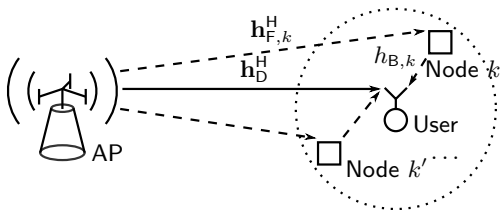
	Backscatter	Ambient backscatter	Symbiotic radio	RIS	RISscatter
Information link(s)	Backscatter	Coexisting	Coexisting	Primary	Coexisting
Primary on backscatter	Carrier	Multiplicative interference	Spreading code	—	Energy uncertainty
Backscatter on primary	—	Multiplicative interference	Channel uncertainty	Passive beamforming	Dynamic passive beamforming
Cooperative devices	—	No	Transmitter and receiver	—	Transmitter, nodes, and receiver
Sequential decoding	—	No	Primary-to-backscatter	—	Backscatter-to-primary
Reflection pattern by	Information source	Information source	Information source	Channel	Source, channel, and priority
Input distribution	Equiprobable	Equiprobable	Equiprobable or Gaussian	Degenerate	Flexible
Load-switching speed	Fast	Slow	Slow	Quasi-static	Arbitrary



- **Primary link:** active legacy transmission from an RF source
- **Backscatter link:** passive free-ride transmission from RISscatter nodes

RISscatter renders the node input distribution as a function of information source, Channel State Information (CSI), and priority of coexisting links.

## Signal model



Within each backscatter block, received signal at primary block  $n$  is

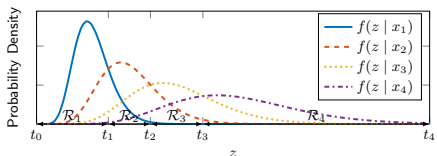
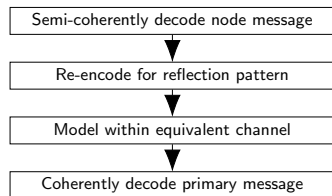
$$y[n] = \mathbf{h}_D^H + \underbrace{\sum_k \alpha_k \mathbf{h}_{C,k}^H \mathbf{x}_k \mathbf{w} \mathbf{s}[n]}_{\mathbf{h}^H(\mathbf{x}_k)} + v[n],$$

### Properties

- ① Primary and backscatter symbols are superimposed by double modulation
- ② Backscatter signal is much weaker due to double fading
- ③ The spreading factor (i.e., symbol period ratio  $N$ ) is usually large
- ④ Each state is simultaneously part of information and beamforming codeword
- ⑤ Reflection pattern over time is guided by input probability distribution

# Low-Complexity Receiver

We propose a low-complexity receiver that exploits the aforementioned properties to avoid Successive Interference Cancellation (SIC).



- Accumulated receive energy  $z = \sum_n |y[n]|^2$  follows Gamma distribution
- Backscatter detection** under primary uncertainty is part of **channel training**
- Requires one energy comparison and re-encoding per backscatter symbol (much simpler than symbiotic radio with  $N$  SIC and 1 combining)

## Joint beamforming, input distribution, and energy detector design

### Achievable rate

$$\sum_k R_{B,k} = \sum_{m_K} P_K(x_{m_K}) \sum_{m'_K} P(\hat{x}_{m'_K} | x_{m_K}) \log P(\hat{x}_{m'_K} | x_{m_K}) / P(\hat{x}_{m'_K})$$
$$R_P = \sum_{m_K} P_K(x_{m_K}) N \log \left( 1 + \frac{|\mathbf{h}^H(x_{m_K})\mathbf{w}|^2}{\sigma_w^2} \right)$$

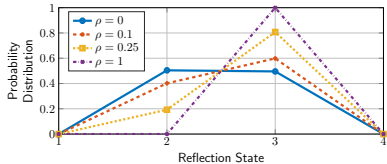
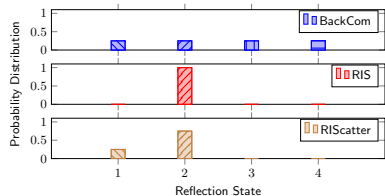
### Problem formulation

$$\max_{\{\mathbf{p}_k\}, \mathbf{w}, \mathbf{t}} \quad \rho R_P + (1 - \rho) \sum_k R_{B,k}$$
$$\text{s.t.} \quad \mathbf{1}^T \mathbf{p}_k = 1, \quad \mathbf{p}_k \geq \mathbf{0}, \quad \forall k,$$
$$t_{l-1} \leq t_l, \quad t_l \geq 0, \quad \forall l,$$
$$\|\mathbf{w}\|^2 \leq P,$$

### Solution by Block Coordinate Descent (BCD)

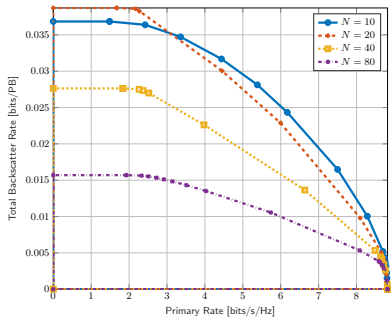
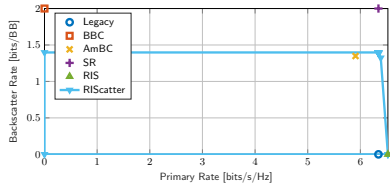
- Input distribution  $\{\mathbf{p}_k\}$ : Karush-Kuhn-Tucker (KKT)
- Active beamforming  $\mathbf{w}$ : Projected Gradient Ascent (PGA)
- Energy decision threshold  $\mathbf{t}$ : Dynamic Programming (DP)

## Simulation results: Input distribution



- BackCom and RIS are special cases of RISscatter with uniform and degenerate input distribution
- Increasing  $\rho$  from 0 to 1 creates a smooth transition from backscatter modulation to passive beamforming

## Simulation results: Rate region



- RISscatter backscatter rate is lower than symbiotic radio (due to energy detection) but higher than ambient backscatter (due to adaptive encoding)
- A large spreading factor  $N$  improves backscatter BER but reduces data rate
- Active and passive transmission can share resource with mutual benefits

# Channel shaping using RIS: From diagonal model to beyond

## Overview

- *What does this paper study?*

To what extent can a passive RIS redistribute the singular values of a Multiple-Input Multiple-Output (MIMO) channel.

- *How does it differ from previous work?*

We consider a Beyond-Diagonal (BD) architecture, depict the singular value region, derive analytical bounds, and solve the rate maximization problem.

- *What are the benefits?*

Channel shaping is ubiquitous for communication, sensing, and power transfer, which helps to decouple the RIS-transceiver design. We also propose an efficient and universal BD-RIS design framework.

# Wave scattering model

## Diagonal RIS

Each element acts as an individual scatterer with phase shift only

$$\boldsymbol{\Theta} = \text{diag}(\theta_1, \dots, \theta_{N_S}) = \text{diag}(e^{j\phi_1}, \dots, e^{j\phi_{N_S}})$$

## BD-RIS

Each group contains  $L$  connected elements, allowing amplitude and phase control

$$\boldsymbol{\Theta} = \text{diag}(\boldsymbol{\Theta}_1, \dots, \boldsymbol{\Theta}_G), \quad \boldsymbol{\Theta}_g^H \boldsymbol{\Theta}_g = \mathbf{I}_L, \quad \forall g$$

- *Subchannel rearrangement*: allows each group to rearrange and combine the backward and forward subchannels by strength

$$\sum_{n=1}^{N_S} |h_{B,n}| |h_{F,n}| \rightarrow \sum_{g=1}^G \sum_{l=1}^L |h_{B,\pi_{B,g}(l)}| |h_{F,\pi_{F,g}(l)}|$$

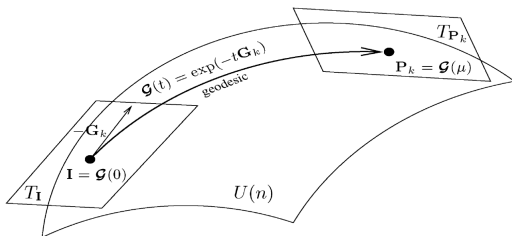
- *Subspace alignment*: rotate backward-forward (intra-group, multiplicative) and direct-indirect (inter-group, additive) singular vectors

$$\mathbf{H} = \overbrace{\mathbf{H}_D + \sum_g \mathbf{U}_{B,g} \boldsymbol{\Sigma}_{B,g} \underbrace{\mathbf{V}_{B,g}^H \boldsymbol{\Theta}_g \mathbf{U}_{F,g}}_{\text{backward-forward}} \boldsymbol{\Sigma}_{F,g} \mathbf{V}_{F,g}^H}^{\text{direct-indirect}}$$

## Some concepts in differential geometry

The feasible domain of  $\Theta_g$  is a unitary Lie group  $U(L)$  with Lie algebra  $\mathfrak{u}(L)$ .

- *Geodesic*: shortest path between two points on a manifold
- *Lie group*: a group that is also a differentiable manifold
- *Lie algebra*: tangent space of Lie group at the identity element



A geodesic emanating from the identity with velocity  $\mathbf{D} \in \mathfrak{u}(L)$  can be described by the exponential map

$$\mathbf{G}_I(\mu) = \exp(\mu\mathbf{D})$$

# Geodesic RCG via Lie algebra

## Non-geodesic vs geodesic Riemannian Conjugate Gradient (RCG)

- Non-geodesic: add then retract

$$\bar{\Theta}_g^{(r+1)} = \Theta_g^{(r)} + \mu \mathbf{D}_g^{(r)}, \quad \Theta_g^{(r+1)} = \bar{\Theta}_g^{(r+1)} (\bar{\Theta}_g^{(r+1)\text{H}} \bar{\Theta}_g^{(r+1)})^{-1/2}$$

- Geodesic: multiplicative and rotational update

$$\Theta_g^{(r+1)} = \mathbf{G}_g^{(r)}(\mu) = \exp(\mu \mathbf{D}_g^{(r)}) \Theta_g^{(r)}$$

## Performance comparison

RCG path	$N_S = 16$			$N_S = 256$		
	Objective	Iterations	Time [s]	Objective	Iterations	Time [s]
Geodesic	$4.359 \times 10^{-3}$	11.59	$1.839 \times 10^{-2}$	$1.163 \times 10^{-2}$	25.58	3.461
Non-geodesic	$4.329 \times 10^{-3}$	30.92	$5.743 \times 10^{-2}$	$1.116 \times 10^{-2}$	61.40	13.50

# Singular value redistribution: Optimization approach

## Pareto frontier of singular values

$$\begin{aligned} \max_{\Theta} \quad & \sum_n \rho_n \sigma_n(\mathbf{H}) \\ \text{s.t.} \quad & \Theta_g^H \Theta_g = \mathbf{I}, \quad \forall g, \end{aligned}$$

## Solution by group-wise geodesic RCG

- Faster convergence thanks to appropriate parameter space
- Step size  $\mu$  can be obtained by the Armijo rule
- Doubling  $\mu$  is computationally efficient  $\exp(2\mu \mathbf{D}_g^{(r)}) = \exp^2(\mu \mathbf{D}_g^{(r)})$

# Singular value redistribution: Analysis approach

## Proposition (Degree of freedom)

*In point-to-point MIMO, BD-RIS cannot achieve a higher Degree of Freedom (DoF) than diagonal RIS.*

## Proposition (Rank-deficient channel)

*If the forward or backward channel is rank- $k$  ( $k \leq N$ ), then regardless of the passive RIS size and architecture, the  $n$ -th singular value of the equivalent channel is bounded by*

$$\begin{aligned}\sigma_n(\mathbf{H}) &\leq \sigma_{n-k}(\mathbf{T}), & \text{if } n > k, \\ \sigma_n(\mathbf{H}) &\geq \sigma_n(\mathbf{T}), & \text{if } n < N - k + 1,\end{aligned}$$

where

$$\mathbf{T}\mathbf{T}^H = \begin{cases} \mathbf{H}_D(\mathbf{I} - \mathbf{V}_F\mathbf{V}_F^H)\mathbf{H}_D^H, & \text{if } \text{rank}(\mathbf{H}_F) = k, \\ \mathbf{H}_D^H(\mathbf{I} - \mathbf{U}_B\mathbf{U}_B^H)\mathbf{H}_D, & \text{if } \text{rank}(\mathbf{H}_B) = k, \end{cases}$$

and  $\mathbf{V}_F$  and  $\mathbf{U}_B$  are the right and left compact singular matrices of  $\mathbf{H}_F$  and  $\mathbf{H}_B$ , respectively.

## Proposition (Unitary RIS without direct link)

*If the BD-RIS is unitary and the direct link is absent, then the channel singular values can be manipulated up to*

$$\text{sv}(\mathbf{H}) = \text{sv}(\mathbf{BF}),$$

where  $\mathbf{B}$  and  $\mathbf{F}$  are arbitrary matrices with the same singular values as  $\mathbf{H}_B$  and  $\mathbf{H}_F$ , respectively,

# Achievable rate maximization

## Problem formulation

$$\begin{aligned} \max_{\mathbf{W}, \Theta} \quad & R = \log \det \left( \mathbf{I} + \frac{\mathbf{W}^H \mathbf{H}^H \mathbf{H} \mathbf{W}}{\eta} \right) \\ \text{s.t.} \quad & \|\mathbf{W}\|_F^2 \leq P, \\ & \Theta_g^H \Theta_g = \mathbf{I}, \quad \forall g. \end{aligned}$$

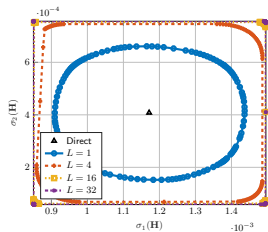
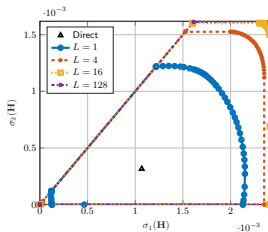
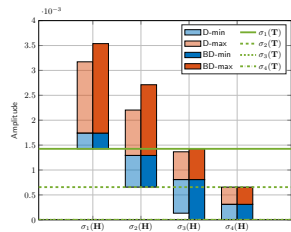
## Local-optimal solution: BCD

- Passive beamforming  $\Theta$ : group-wise geodesic RCG
- Active beamforming  $\mathbf{W}$ : eigenmode transmission and water-filling

## Low-complexity solution: two-stage

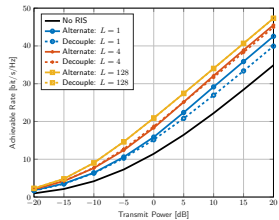
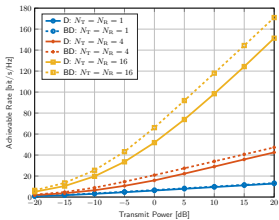
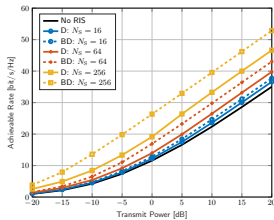
- Shaping stage: channel power gain maximization, solved in closed form
- Transmission stage: eigenmode transmission and water-filling

# Simulation results: Singular value

(a)  $2 \times 32 \times 2$ (b)  $2 \times 128 \times 2$ (c)  $4 \times 32 \times 4$  (rank-1)

- BD-RIS provides 22% and 38% dynamic range gain for  $\sigma_1(\mathbf{H})$  and  $\sigma_2(\mathbf{H})$
- Increasing group size enlarges singular value region with better trade-off
- Asymptotic bounds in rank-deficient channels are valid for both architectures

# Simulation results: Achievable rate

(a)  $4 \times 128 \times 4$ (b)  $N_T \times 128 \times N_R$ (c)  $4 \times N_S \times 4$ 

- Deficit from low-complexity design vanishes as RIS evolves towards unitary
- BD-RIS can activate multiple streams at lower transmit power
- Percentage rate gain of BD-RIS scales with MIMO dimension and group size

## Future works: I

### Coherent RISscatter detector

$$y[n] = \mathbf{h}_D^H + \mathbf{h}_C^H x \mathbf{w} s[n] + v[n],$$

- Same model as index modulation
- $x$  has finite support  $\rightarrow y[n]$  is a Gaussian mixture (non-elementary entropy)
- Achievable rate can be approximated as

$$R_B = \sum_i p(x_i) \log \sum_j p(x_j) \frac{4\sigma_i^2 \sigma_j^2}{(\sigma_i^2 + \sigma_j^2)^2}$$

- Bit Error Rate (BER) performance?
- Code-domain Non-Orthogonal Multiple Access (NOMA)?

## Future works: II

### Multiplicative broadcast channel

The received signal is

$$y_k = h_k \prod_q x_q + n.$$

- SIC → successive channel refinement (better symbol-level precoding)
- Log-normal is also maximum entropy distribution
- Product of log-normal is log-normal

Index modulation is a special case with superuser  $R = R_1 + R_2$

- $x_1 \sim \mathcal{CN}(0, \sigma_1^2)$  and  $x_2$  with finite support
- Index message encoded in the Euclidean distance between  $hx_2^{(i)}$
- Decode  $x_2$  first, rate depends on entropy of Gaussian mixture

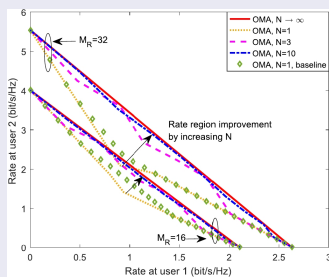
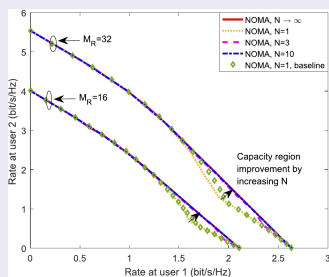
## Future works: III

### Rate splitting × index modulation

The received signal is

$$y_k = h_k \theta \sum_q x_q + n.$$

- Dynamic RIS achieves the convex hull below by time-sharing [7]



- Common message can be embedded in  $\theta$  to push the boundary

## Future works: IV

## Feasibility of interference alignment by RIS

$$\begin{aligned} \text{find } \quad & \Theta \\ \text{s.t. } \quad & \mathbf{H}^{[kj]} = \mathbf{H}_{\text{D}}^{[kj]} + \mathbf{H}_{\text{B}}^{[k]} \Theta \mathbf{H}_{\text{F}}^{[j]} = \mathbf{0}, \quad \forall j \neq k \\ & \text{rank}(\mathbf{H}^{[kk]}) = d_k, \quad \forall k \end{aligned}$$

- Necessary and sufficient feasibility conditions?
- How many scattering elements are required on expectation?
- Multi-sector BD-RIS [8]?

-  Q. Wu and R. Zhang, "Towards smart and reconfigurable environment: Intelligent reflecting surface aided wireless network," *IEEE Communications Magazine*, vol. 58, pp. 106–112, Jan 2020.
-  R. Deng, F. Yang, S. Xu, and M. Li, "A low-cost metal-only reflectarray using modified slot-type phoenix element with 360° phase coverage," *IEEE Transactions on Antennas and Propagation*, vol. 64, pp. 1556–1560, Apr 2016.
-  S. Hu, C. Liu, Z. Wei, Y. Cai, D. W. K. Ng, and J. Yuan, "Beamforming design for intelligent reflecting surface-enhanced symbiotic radio systems," in *ICC 2022 - IEEE International Conference on Communications*, May 2022, pp. 2651–2657.
-  E. Arslan, I. Yildirim, F. Kilinc, and E. Basar, "Over-the-air equalization with reconfigurable intelligent surfaces," *IET Communications*, vol. 16, pp. 1486–1497, Aug 2022.
-  M. Trotter, J. Griffin, and G. Durgin, "Power-optimized waveforms for improving the range and reliability of RFID systems," in *2009 IEEE International Conference on RFID*, Apr 2009, pp. 80–87.
-  B. Molina-Farrugia, A. Rivadeneyra, J. Fernández-Salmerón, F. Martínez-Martí, J. Banqueri, and M. A. Carvajal, "Read range

enhancement of a sensing RFID tag by photovoltaic panel," *Journal of Sensors*, vol. 2017, pp. 1–7, 2017.

-  X. Mu, Y. Liu, L. Guo, J. Lin, and N. Al-Dhahir, "Capacity and optimal resource allocation for IRS-assisted multi-user communication systems," *IEEE Transactions on Communications*, vol. 69, pp. 3771–3786, Jun 2021.
-  H. Li, S. Shen, and B. Clerckx, "Beyond diagonal reconfigurable intelligent surfaces: A multi-sector mode enabling highly directional full-space wireless coverage," *IEEE Journal on Selected Areas in Communications*, vol. 41, pp. 2446–2460, Aug 2023.